2023 IEEE 34th Annual International Symposium on Personal, Indoor and Mobile Radio Communications (PIMRC) | 978-1-6654-6483-3/23/$31.00 ©2023 IEEE | DOI: 10.1109/PIMRC56721.2023.10293899

# TDoA and Monostatic Radar Data Fusion for Single Object Localization and Tracking

1st Evert I. Pocoma Copa
*Université libre de Bruxelles (ULB)*
Brussels, Belgium
epocomac@ulb.be

2nd Cédric Hannotier
*Université libre de Bruxelles (ULB)*
Brussels, Belgium
cedric.hannotier@ulb.be

3rd François Quitin
*Université libre de Bruxelles (ULB)*
Brussels, Belgium
fquitin@ulb.be

4th Luc Vandendorpe
*Université catholique de Louvain (UCLouvain)*
Ottignies-Louvain-la-Neuve, Belgium
luc.vandendorpe@uclouvain.be

5th Philippe De Doncker
*Université libre de Bruxelles (ULB)*
Brussels, Belgium
philippe.dedoncker@ulb.be

6th François Horlin
*Université libre de Bruxelles (ULB)*
Brussels, Belgium
francois.horlin@ulb.be

***Abstract*—In this paper, we present the fusion of passive Time-Difference-of-Arrival (TDoA) and active monostatic radar measurements in the context of single object localization and tracking. We assume a target equipped with a wireless transmitter so that the passive-TDoA and active-radar sensors can simultaneously detect it. For the localization problem, we base our approach on the Constrained-Weighted-Least-Squares (CWLS) method, which has better accuracy than the Least-Squares (LS) and Weighted-LS approaches. Nevertheless, CWLS suffers from estimation bias when the measurement noise is large. We show that it is possible to reduce such a bias by using both TDoA and monostatic radar measurements. For the tracking problem, we base our approach on Bayesian filtering. Therefore, we detail the TDoA, radar and combined measurement models required for the filtering process regardless of the Bayesian Filter implementation. We show that the combined measurements result in enhanced tracking capabilities, e.g., improved reliability and larger tracking area compared to the radar-only case. In addition, we present other possible combinations of radar and TDoA measurements that one could encounter in practical scenarios. Finally, we present experimental results to validate and support our work.**

***Index Terms*—TDoA, radar, sensor fusion, CWLS, Localization, Tracking.**

## I. Introduction

Localization and tracking play an important role in current applications such as traffic control, surveillance, autonomous driving, etc. In fact, they are not problems fully independent from each other. For instance, localization is used in the initialization stage of any tracking application, which can be critical in some cases leading to several issues, such as increased number of false tracks or divergence of the filter [1]. In addition, one could classify the localization/tracking approaches into passive or active. On the one hand, passive approaches do not interact with the target and have become important in wireless networks. For instance, positioning reference signals (PRS) are included in the protocols to support device localization based on the estimation of the signal Time of Arrival (ToA) [2]. On the other hand, active approaches use extra useful information by interacting directly with the target. For instance, active radar sensors measure directly the target kinematics. In that respect, this paper is an attempt to show the data-fusion benefits of two specific passive and active sensors such as Time Difference of Arrival (TDoA) and monostatic radar.

TDoA measurements are used to estimate the transmitter position when it is not time-synchronized to the infrastructure, which is usually the case in wireless networks. Consequently, a linear system is constructed by squaring and rearranging the TDoA measurements considering time offset and transmitter position as unknown variables [3]. That linear system is traditionally solved using the Weighted Least Squares (WLS) method; however, the estimates are imprecise and sensitive to noise. Another approach is the Constrained Weighted Least Squares (CWLS) that includes an additional constraint based on the target position and its distance to the reference Base Station (BS) [4]. This approach greatly improves the precision but reduces the accuracy, since bias is introduced to the system due to several reasons such as large noise, unknown weighting matrix, intrinsic non-linearity of the problem, etc., [5]. Therefore, as it will be shown later on, TDoA approaches alone do not provide reliable estimates.

Current active-radar sensors have become popular in many applications due to their improved range resolution (up to the centimeter scale in Frequency Modulated Continuous Wave (FMCW) radars) and angle measurements capabilities (multi-antenna radar) [6]. Nevertheless, radars have a limited Field of View (FoV) that limits their use only to their surroundings. Such a FoV depends on different aspects such as transmit power, antenna gains, radar cross-section, etc. Moreover, it might be a limiting factor when part of the target trajectory happens outside the radar FoV.

On the one hand, multiple fusion approaches involving passive TDoA with other passive sensors have been proposed in the literature [7], [8], [9], [10]. For instance in [7], TDoA and Frequency Difference of Arrival (FDoA) are combined as a way to estimate not only the target position but also its velocity. In [8], [9], the use of TDoA and Angle of Arrival (AoA) is addressed to improve localization accuracy. Additionally in [10], both FDoA and AoA are used together with TDoA to combine their already mentioned advantages. On the other hand, active radars and TDoA are combined in [11]. More precisely, TDoA and FDoA are purely estimated from the multistatic radar signals and not from a different sensor. Later, those estimates are used to estimate the target kinematics using the WLS method. Nevertheless, the fusion between passive TDoA and active radars has been somehow overlooked in both theoretical and practical studies.

In this paper we address the fusion of TDoA and monostatic radar measurements for single-object localization and tracking. Therefore the contributions of this paper are threefold:

- We build a unified model for the localization using both TDoA and active monostatic radar measurements. We rely on the CWLS method and show that such a fusion approach can help to greatly reduce the estimation bias inherent to the method.
- We describe the necessary steps to combine TDoA and active monostatic radar measurements for tracking applications. We show that the benefit of such a fusion is to reach the accuracy delivered by the radar while ensuring the track continuity thanks to the TDoA technology.
- Lastly, we present experimental results to validate our analysis. We consider not only common fusion cases but also other interesting measurement combinations that could arise in practical scenarios, where a single technology is not necessarily sufficient to localize a device. For instance, TDoA and range only, or TDoA of only three BSs and radar range only, etc.

## II. System Model

For the sake of simplicity, we consider that all sensors are placed in a 2D plane. We assume that a target is detected by a monostatic radar and is equipped with a wireless transmitter that emits beacons at a regular basis. With such considerations, we proceed to describe the TDoA and radar models separately.

### A. TDoA model

The transmitter beacons are received at M time-synchronized BSs. Each BS-i, located at the known position $\mathbf{s}_i (i = 1, 2, ...M)$, measures the transmitter beacon ToA. The transmitter is located at an unknown position $\mathbf{u} = [x, y]^T$ inside the area delimited by the BSs. Notice that the transmitter is not time-synchronized with the BSs. Thus, the ToA measurements include a common yet unknown time offset $\tau$, which is removed by using TDoA measurements. Notice that a Range Difference of Arrival (RDoA) measurement is equal to the TDoA multiplied by the propagation velocity $c$. Therefore, we refer to RDoA and TDoA measurements interchangeably herein.

The TDoA measurement for BS-i and BS-1 is defined as:

$$r_{i,1} = (r_i + d_0) - (r_1 + d_0) + n_{i,1}, \quad i = 2, 3, ..., M \tag{1}$$

where $r_i = \|\mathbf{u} - \mathbf{s}_i\|$, $d_0 = c\tau$ and $n_{i,1} = n_i - n_1$, with $n_i$ being the ToA-measurement noise at BS-$i$.

By taking the square of (1) and rearranging the terms as done in [5], [3], we obtain:

$$r_{i,1}^2 + \|\mathbf{s}_1\|^2 - \|\mathbf{s}_i\|^2 + 2(\mathbf{s}_i - \mathbf{s}_1)^T\mathbf{u} + 2r_{i,1}r_1 = 2r_1 n_{i,1} + n_{i,1}^2. \tag{2}$$

Such an expression is known as the TDoA error equation and has the advantage of being linear in $\mathbf{u}$ and $r_1$. In order to use the CWLS approach, (2) is rearranged as follows:

$$r_{i,1}^2 - \|\mathbf{s}_i - \mathbf{s}_1\|^2 + 2(\mathbf{s}_i - \mathbf{s}_1)^T(\mathbf{u} - \mathbf{s}_1) + 2r_{i,1}r_1 = 2r_1 n_{i,1}. \tag{3}$$

Notice that the second-order noise term $n_{i,1}^2$ is neglected considering a sufficiently high SNR, which is a common practice in the literature [5].

The resulting linear system of equations is constructed by gathering all TDoA measurements as:

$$\mathbf{h}_T - \mathbf{G}_T\boldsymbol{\theta}_T = \mathbf{B}_T\mathbf{n}_T, \tag{4}$$

with the unknown vector $\boldsymbol{\theta}_T = [(\mathbf{u} - \mathbf{s}_1)^T r_1]^T$ and matrices

$$\mathbf{h}_T = \begin{bmatrix} r_{2,1}^2 - \|\mathbf{s}_2 - \mathbf{s}_1\|^2 \\ \vdots \\ r_{M,1}^2 - \|\mathbf{s}_M - \mathbf{s}_1\|^2 \end{bmatrix}, \mathbf{G}_T = -2\begin{bmatrix} (\mathbf{s}_2 - \mathbf{s}_1)^T & r_{2,1} \\ \vdots & \vdots \\ (\mathbf{s}_M - \mathbf{s}_1)^T & r_{M,1} \end{bmatrix}$$

$\mathbf{B}_T = 2diag([r_2 \dots r_M])$ and $\mathbf{n}_T = [n_{2,1} \dots n_{M,1}]^T$. The TDoA noise vector $\mathbf{n}_T$ is assumed to be Gaussian distributed with zero mean and covariance matrix $\mathbf{Q}_T = diag([\sigma_2^2 \dots \sigma_M^2]) + \sigma_1^2 \mathbf{1}_{M-1}\mathbf{1}_{M-1}^T$, where $\sigma_i^2$ and $\mathbf{1}_{M-1}$ are the ToA-noise variances and (M-1)-dimensional all-one vector, respectively [12], [13].

### B. Radar model

We consider a monostatic radar equipped with a linear-antenna array at the receiver located at $\mathbf{s}_R = [x_R, y_R]^T$. It provides the detected target range $r_R$ and radial velocity $v_R$ and azimuth angle $\alpha_R$. That is, we assume the radar data at the radar detection output. Similarly to [14], the radar data $r_R$, $v_R$ and $\alpha_R$ can be expressed as:

$$\begin{aligned} r_R &= \|\mathbf{u} - \mathbf{s}_R\| + n_r \quad ; \quad v_R = \langle \mathbf{v}, \mathbf{u}_r \rangle + n_v \\ \alpha_R &= \arctan(\frac{y - y_R}{x - x_R}) + n_\alpha \end{aligned} \tag{5}$$

where $\mathbf{v} = [v_x, v_y]^T$ is the target velocity; $(\langle . \rangle)$ denotes the inner product and $\mathbf{u}_r$ is a radial unitary vector defined as $\mathbf{u}_r = \frac{\mathbf{u} - \mathbf{s}_R}{\|\mathbf{u} - \mathbf{s}_R\|}$. All additive noise terms, $n_r$, $n_v$ and $n_\alpha$, are assumed mutually independent Gaussian distributed with zero mean and variances $\sigma_r^2$, $\sigma_v^2$ and $\sigma_\alpha^2$, respectively. Notice that the radar only detects the target when this is inside its FoV, that is defined as $FoV := \{(r_R, \alpha_R) | r_R \leq r_{max} \wedge -\phi_{max} \leq \alpha_R - \frac{\pi}{2} \leq \phi_{max}\}$, where $r_{max}$ and $\phi_{max}$ are maximum range and angle values viewed from the radar.

## III. Localization

### A. TDoA - Localization

The system of equations (4) can be solved using the WLS method [3]. However, the CWLS approach is usually more accurate at a cost of introducing bias in the system [4],

[5]. In short, $\boldsymbol{\theta}_T$ can be estimated by solving the following constrained optimization problem:

$$\begin{aligned}\hat{\boldsymbol{\theta}}_T = \min_{\boldsymbol{\theta}_T} \quad & (\mathbf{h}_T - \mathbf{G}_T\boldsymbol{\theta}_T)^T \mathbf{W}_T (\mathbf{h}_T - \mathbf{G}_T\boldsymbol{\theta}_T) \\ \text{s.t.} \quad & \boldsymbol{\theta}_T^T \boldsymbol{\Sigma} \boldsymbol{\theta}_T = 0\end{aligned} \tag{6}$$

with $\mathbf{W}_T = (\mathbf{B}_T \mathbf{Q}_T \mathbf{B}_T)^{-1}$ and $\boldsymbol{\Sigma} = diag([1, 1, -1])$. Notice that the constraint comes from the fact that $r_1^2 = (\mathbf{u} - \mathbf{s}_1)^T(\mathbf{u} - \mathbf{s}_1)$. An efficient yet iterative way to solve (6) was introduced in [4]. Notice that $\mathbf{B}_T$ is initially unknown, and thus it is initialized as an identity matrix and reevaluated at each CWLS-iteration.

### *B. Radar - Localization*

The target position $\mathbf{u}$, using only radar, can be computed:

$$\mathbf{u} = r_R\ [\cos(\alpha_R)\ \ \sin(\alpha_R)]^T + \mathbf{s}_R. \tag{7}$$

Notice that such an estimation is a trivial conversion of Polar to Cartesian coordinates. However, the fusion of radar and TDoA data is not straightforward.

### *C. TDoA and Radar - Localization*

To merge both sensor data into a single system of equations, we perform the following two steps. First, we use the AoA-linear approximation introduced in [8], [9] as:

$$[\sin(\alpha_R)\ -\cos(\alpha_R)](\mathbf{u} - \mathbf{s}_R) = r_R n_r. \tag{8}$$

Second, we constrain the radar to be located at the same location as the reference-BS, i.e., $\mathbf{s}_R = \mathbf{s}_1$. Rearranging the terms to have an unknown vector $\boldsymbol{\theta}_R = [(\mathbf{u} - \mathbf{s}_R)^T r_R]^T$ results into the following radar linear system of equations:

$$\mathbf{h}_R - \mathbf{G}_R\boldsymbol{\theta}_R = \mathbf{B}_R\mathbf{n}_R, \tag{9}$$

with vectors $\mathbf{h}_R = [0\, r_R]^T$, $\mathbf{n}_R = [n_\alpha\, n_r]^T$ and matrices

$$\mathbf{G}_R = \begin{bmatrix} -\sin(\alpha_R) & \cos(\alpha_R) & 0 \\ 0 & 0 & 1 \end{bmatrix}, \mathbf{B}_R = \begin{bmatrix} r_R & 0 \\ 0 & 1 \end{bmatrix}.$$

Notice that (9) is an undetermined system of equations due to the increase in unknown variables compared to (7).

Lastly, a joint TDoA-radar system of equations can be constructed by concatenating (4) and (9). Consequently, the unknown vector $\boldsymbol{\theta} = \boldsymbol{\theta}_T = \boldsymbol{\theta}_R$ can be estimated from

$$\begin{aligned}\hat{\boldsymbol{\theta}} = \min_{\boldsymbol{\theta}} \quad & (\mathbf{h} - \mathbf{G}\boldsymbol{\theta})^T \mathbf{W} (\mathbf{h} - \mathbf{G}\boldsymbol{\theta}) \\ \text{s.t.} \quad & \boldsymbol{\theta}^T \boldsymbol{\Sigma} \boldsymbol{\theta} = 0\end{aligned} \tag{10}$$

with $\mathbf{h} = [\mathbf{h}_T^T\, \mathbf{h}_R^T]^T$, $\mathbf{G} = [\mathbf{G}_T^T\, \mathbf{G}_R^T]^T$, $\mathbf{W} = (\mathbf{B}\,\mathbf{Q}\,\mathbf{B})^{-1}$ and block-diagonal matrices $\mathbf{B} = diag(\{\mathbf{B}_T, \mathbf{B_R}\})$, $\mathbf{Q} = diag(\{\mathbf{Q}_T, \sigma_\alpha^2, \sigma_r^2\})$.

Notice that (10) has the same form as (6); hence the CWLS-iterative approach can also be used to find the solution. In addition, we would like to highlight two benefits of using this approach.

- First, the bias due to the use of CWLS-approach is reduced, since $\mathbf{B}$ is partially known at the first CWLS iteration. This is not the case for the TDoA-CWLS in (6), where $\mathbf{B}_T$ is completely unknown at the first iteration.
- Second, such an approach simplifies the analysis for different TDoA and radar combinations, as it will be described in Section V-B. Lastly, the constraint imposed on the radar position, i.e., $\mathbf{s}_R = \mathbf{s}_1$, can be lifted by adding a second radar; however, such an approach is not presented in this work.

## IV. Tracking

Single Object Tracking (SOT) is usually accomplished by means of Bayesian filtering, which is mainly composed of a prediction step followed by a correction step. Since the main focus of this paper is to show the benefits of TDoA-radar fusion, we detail only the process and measurement models to be used, rather than to describe the Bayesian filtering in detail. In addition, we refer the reader to [15] for specific details about the implementation of Bayesian filtering approaches.

### *A. Process Model*

Similar to Section III, we assume a single target/transmitter in the scene. Therefore, we define $\mathbf{x} = [x\,\dot{x}\,y\,\dot{y}]^T$ as the state vector, where $(x, y)$ and $(\dot{x}, \dot{y})$ are the target Cartesian position and velocity, respectively. The state vector at time instant $k+1$ can be deduced from the previous time instant $k$ as $\mathbf{x}_{k+1} = \mathbf{A}_k\mathbf{x}_k + \mathbf{w}_k$, where $\mathbf{A}_k$ is the transition matrix and $\mathbf{w}_k$ is a zero-mean Gaussian-noise vector with covariance matrix $\boldsymbol{\Sigma}_k$. $\mathbf{A}_k$ and $\boldsymbol{\Sigma}_k$ are given by the chosen process model (e.g., Constant Velocity Model (CVM), Constant Acceleration Model (CAM), etc.). We kindly refer the reader to [16] for more details on such process models.

### *B. Measurement Model*

It defines a mapping from the state space to the measurement space, i.e., $\mathbf{z}_k = g(\mathbf{x}_k) + \mathbf{v}_k$, where $\mathbf{z}$ and $g(.)$ are the measurement vector and function, respectively. $\mathbf{v}_k$ is a zero-mean Gaussian noise vector with covariance matrix $\mathbf{Q}_k$. Notice that $g(.)$ and $\mathbf{Q}_k$ are defined by the type of available sensors at a specific time instant $k$. Therefore, we define $g(.)$ and $\mathbf{Q}_k$ for the possible scenarios.

*1) TDoA model:* All available TDoA measurements defined in (1) are gathered resulting in

$$g_T(\mathbf{x}_k) = [r_{2,1}(\mathbf{x}_k)\ \ldots\ r_{M,1}(\mathbf{x}_k)]^T \tag{11}$$

and the measurement covariance matrix $\mathbf{Q}_k = \mathbf{Q}_{T,k}$ as defined in Section II-A. Notice that $\mathbf{x}_k$ is explicitly written to highlight the dependence of $r_{i,1}$ on $\mathbf{x}_k$.

*2) Radar model:* All radar measurements, defined in (5), are gathered as

$$g_R(\mathbf{x}_k) = [r_R(\mathbf{x}_k)\, v_R(\mathbf{x}_k)\, \alpha_R(\mathbf{x}_k)]^T, \tag{12}$$

and the measurement covariance matrix is defined as $\mathbf{Q}_k = \mathbf{Q}_{R,k} = diag([\sigma_r^2, \sigma_v^2, \sigma_\alpha^2])$. Notice that different from the localization case explained in Section III, the radial velocity is also taken into account as an extra measurement.

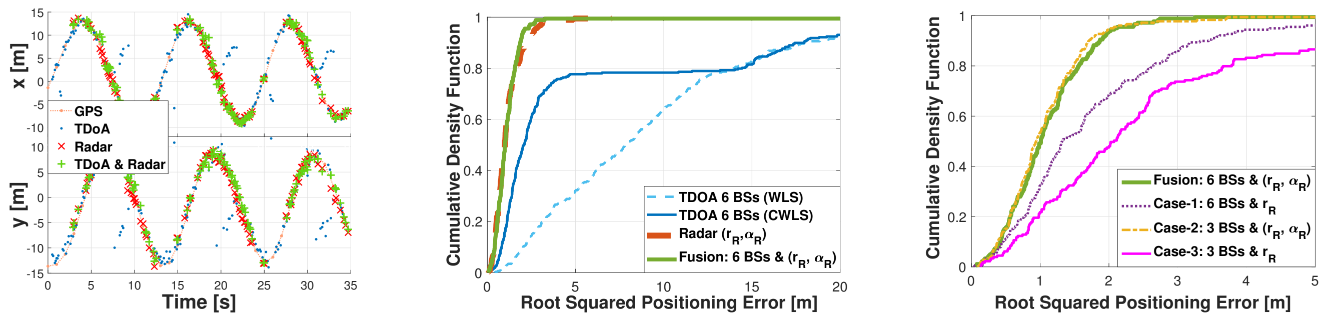


(a) (b) (c)

Fig. 1. Experimental localization results: a) CWLS-estimated x and y-coordinates for a particular realization. Experimental Error-CDF considering all realizations for b) CWLS and WLS methods. c) additional considered scenarios. All Error-CDF curves are computed with only data inside the radar-FoV.

*3) TDoA and Radar model:* When both sensors detect the target, the measurement model is the concatenation of both previous models, i.e., $g(\mathbf{x}_k) = [g_T(\mathbf{x}_k)\, g_R(\mathbf{x}_k)]^T$ with measurement covariance matrix $\mathbf{Q}_k$ being block-diagonal as $\mathbf{Q}_k = diag(\{\mathbf{Q}_{T,k}, \mathbf{Q}_{R,k}\})$. Notice that for the tracking case, the radar is not restricted to be placed at the same location as the reference BS, as it was in the localization case.

## V. Experimental Results

A measurement campaign was conducted in Belgium - Nivelles city. A general overview of the scenario is shown in Fig. 2; where all sensors were placed in a real roundabout. One transmitter is placed on top of a car equipped with a GPS sensor that records the position every second. The car moves in a counterclockwise direction along the roundabout as it is depicted in Fig. 2, where the initial position is denoted by a big-star marker. Notice that our analysis can be extended to a multiple object scenario after addressing the data association problem; however, we analyze only the SOT case to better show the fusion benefits.

The transmitter sends an OFDM-frame every 10 ms over a 20 MHz bandwidth at a 2.35 GHz carrier frequency. The infrastructure is composed of $M = 6$ time-synchronized BSs placed at the positions given in Table I. Each BS samples the received signal at 100 MHz and obtains ToA measurements in two stages as done in [17]. First, a rough ToA estimate is obtained by correlating the received and transmitted signals. Second, a sub-sampled ToA refinement is estimated using a parabolic interpolation around the correlation maxima.

Separately, an off-the-shelf FMCW radar (WR1843BOOST) is placed at the same location as BS-1, with orientation angle $\frac{3}{4}\pi$. The radar-FoV is shown in Fig. 2a as the light-green circular sector. The radar provides detections every $T = 100$ ms; consequently, the ToA measurements are decimated to match the radar data rate. The radar is configured with a single transmitter and 4 receivers enabled, 600 MHz bandwidth, 77 GHz starting frequency, 128 samples per chirp and 128 chirps per frame. The radar detections are computed following the procedure explained in [14]-Section-II-A. Lastly, notice that the target trajectory goes inside and outside the radar-FoV but never leaves the delimited area by the BSs. That is, we are able to collect TDoA measurements all along the target trajectory but not for the radar sensor.

TABLE I
BSs LOCATIONS

| BS-id | 1 | 2 | 3 | 4 | 5 | 6 |
|---|---|---|---|---|---|---|
| $x_i[m]$ | -12.64 | -13.99 | -1.79 | 16.69 | 17.84 | 6.35 |
| $y_i[m]$ | 13.91 | -8.37 | -16.94 | -8.79 | 4.19 | 15.40 |

### A. Localization Results

The transmitter positions are estimated using TDoA, radar and both sensor measurements, as explained in Section III. To compare objectively the different methods, we define the Root Squared Positioning Error (RSPE) as RSPE $= \|\hat{\mathbf{u}} - \mathbf{u}_{GPS}\|$, where $\hat{\mathbf{u}}$ is the estimated position and $\mathbf{u}_{GPS}$ is the position provided by the GPS sensor. Fig.1b and Fig.1c present the RSPE-CDF curves for different cases considering all the realizations. We refer to this curves as error CDF.

We first address the drawback of using TDoA-only approaches. On the one hand, Fig.1b shows that the simplest approach of TDoA-WLS, which solves (6) ignoring the constraint, provides large localization errors. The estimation error increases together with the TDoA-measurement error. As a result, the associated error CDF presents only one mode. On the other hand, TDoA-CWLS provides better estimates for small TDoA-errors, compared to TDoA-WLS; however, the error dramatically increases when the measurement noise is above a certain threshold. As a result, the TDoA-CWLS associated error CDF presents multiple modes at 2 and 17 meters, which puts in evidence the presence of bias in the estimates. Therefore, it is clear that TDoA-measurements alone do not always provide reliable estimates.

We now proceed to highlight the benefits of the fusion. The iterative CWLS approach presents estimation bias, since the weighting matrix $\mathbf{B}_T$ of (6) is completely unknown. Different from the bias reduction algorithm proposed in [5], we propose to use radar measurements to make $\mathbf{B}$ of (10) partially known for the radar part and thus, reducing the bias introduced by the CWLS method. As a result, the radar and fusion error-CDF

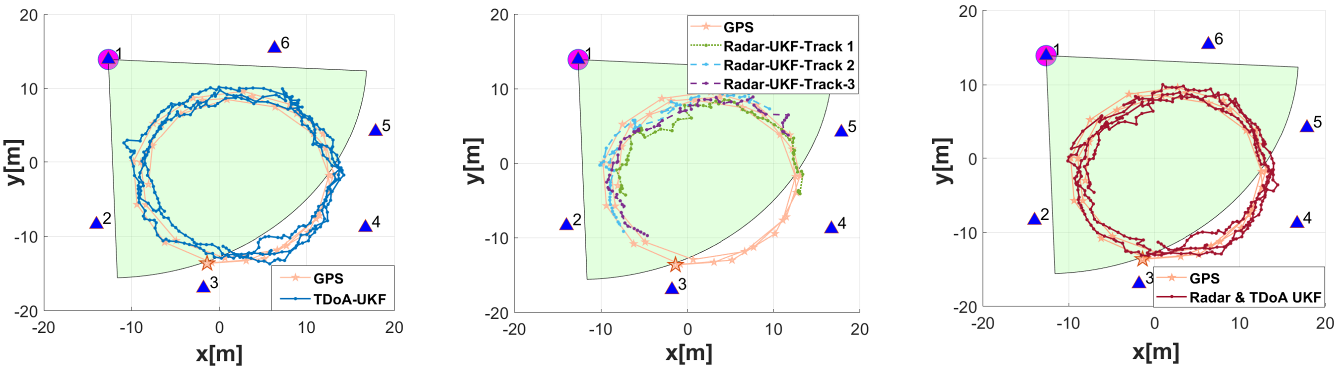


(a) (b) (c)

Fig. 2. Experimental tracking results. In all cases an UKF is implemented a) TDoA-UKF. b) Radar UKF. c) TDoA & Radar UKF. The BSs and radar are represented by the numbered triangles and the purple dot, respectively. Notice that the radar is located at the same location as the reference-BS.

curves in Fig.1b present only one mode, showing that the bias has been vastly removed.

It must be noticed that the fusion for localization is possible whenever both TDoA and radar measurements are available, i.e., only inside the radar FoV. In addition, we present in Fig. 1a the $x$ and $y$-coordinate estimates for a particular realization to better observe the impact of fusion. The bias is evident for the estimates using only TDoA measurements (blue '.'), e.g., at 8, 22, and 33 seconds. The estimates using both TDoA and radar measurements (green '+') present a greatly reduced bias for the same time instants (8, 22, 33 seconds). However, they are only available once the target enters the radar FoV. Whilst the localization results of fusion and radar are quite similar, the fusion strategy could allow tracking in a bigger FoV than the radar-FoV, as it is shown in Section-V-C.

### B. Localization Results for Additional scenarios

There are multiple interesting ways to combine the radar and TDoA measurements. Nevertheless, we analyze only three cases herein:

- *Case 1:* All M=6 BSs and only the radar range $r_R$ are available. Whilst it is enough to use only TDoA measurements to estimate the transmitter position, using TDoA and radar range combined reduces the bias.
- *Case 2:* Only three BSs (1, 3 and 5) are enabled and radar measurements $r_R, \alpha_R$ are provided.
- *Case 3:* Only three BSs (1, 3 and 5) are enabled as in case-2; however, only radar range $r_R$ is available. Notice that localization is not possible with radar alone.

Notice that case-1 and case-3 assume a single antenna mono-static radar. It implies that the hardware and processing requirements are simpler for such type of radars and thus, it could lower the cost of sensor deployment. In case-2 and case-3 localization using TDoA alone might not find a unique solution.

All error-CDF curves for cases 1,2 and 3 are shown in Fig 1c. The error-CDF of fusion is also shown for reference. Notice that all curves are unimodal which indicates a bias reduction thanks to the partially known weighting matrix $\mathbf{B}$. Case-1 performs worse than the fusion since it only uses the radar-range $r_R$ measurement. However, it performs better than TDoA-alone shown in Fig 1b and it does not present a dramatic increase of error. Moreover, case-2 performs the closest to the fusion, which reveals the importance of the radar measurements. Interestingly, case-3 is still able to localize the target with reduced precision.

### C. Tracking results

Since the measurement models are nonlinear as described in Section IV, we implemented the well-known Unscented Kalman Filter (UKF) [15]. We choose the CVM as process model used in the prediction step. We expect the maximum change in velocity during one time interval $T$ to be $\Delta v_{max} = 2$ m/s. Consequently, we set $\sigma_w = \Delta v_{max}/T = 20$ m/$s^2$ that is needed to construct the CVM model [16].

The hyper-parameters needed in the correction step are chosen as follows. Since the TDoA measurements are decimated to match the radar data rate, the remaining ToA samples are used to estimate the ToA-noise variances $\sigma^2_{i,k}$. Due to the car dimensions and radar configuration, the radar detections fall over multiple range/radial-velocity/angle bins. Therefore, instead of setting the noise variances equal to the radar cube resolutions, we empirically set them to the values that work the best in all measurements, that is $\sigma_r = 0.5$ m, $\sigma_v = 2$ m/s and $\sigma_\alpha = 0.0349$ rad.

Notice that no data-association algorithm is used since we study a SOT scenario. We implemented an oversimplified track management approach, since the target enters and leaves the radar FoV. In short, a track is, respectively, accepted or terminated after receiving or missing measurements for five consecutive time instants.

Fig. 3a shows the error-CDF curves of tracking using TDoA, radar and both sensor measurements. The error-CDF using radar is similar to the one using both TDoA and radar; however, the main difference is the track continuity that we

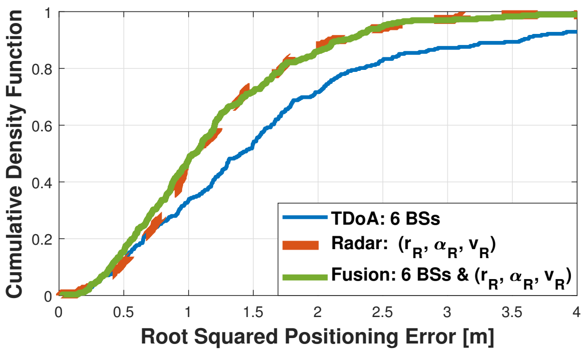


(a)

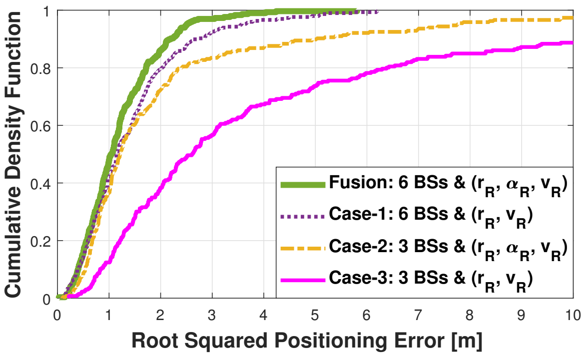


(b)

Fig. 3. Experimental tracking error-CDF considering all realizations for a) TDoA, Radar, and both Fusion; b) additional TDoA-Radar combination cases

explain as follows. Fig. 2 shows the tracking results in the $xy$-plane for a particular realization. Due to the radar FoV, it is not possible to track the target at all times using only radar measurements. Moreover, every time the target enters into the radar FoV, the track management assumes a new identity for the track, as seen in Fig. 2b. Such track-continuity problem is not present in the TDoA case, as shown in Fig. 2a. However, the filter initialization might be inaccurate due to the localization using only TDoA, due to estimation bias as seen in Section V-A. The use of both radar and TDoA measurements eliminates the track continuity problem and reduces the inaccuracy of initialization, as seen in Fig. 2c.

Lastly, Fig. 3b shows the error-CDF curves for the additional cases. The reasoning is similar to the localization case except for two main differences. First, cases 1,2 and 3 perform tracking in the area surrounded by the BSs; whereas in the localization, case 2 and 3 are only possible inside the radar FoV. Second, case 2 no longer performs the closest to the fusion case as in the localization, since tracking outside the radar FoV is done only with only 3 BSs which reduces the performance as shown in Fig. 3b.

## VI. Conclusions

In this work, we described a simple yet effective fusion of TDoA and monostatic radar measurements. We not only addressed the localization but also the tracking application. We highlighted the fusion benefits such as bias reduction in the localization case and track continuity in the tracking application. Experimental results support our claims. Lastly, our future work is directed towards showing the fusion benefits in a multiple object scenario. For instance, high localization bias could lead to wrong/false tracks initialization.

## Acknowledgment

The authors acknowledge the financial support of the Walloon Region through the WIN2Wal/2018/1/DI/34 LUMINET project.

## References

[1] G. Lee, S. Lee, K. Kim, and N. Kwak, "Probabilistic track initiation algorithm using radar velocity information in heavy clutter environments," in *2018 15th European Radar Conference (EuRAD)*, 2018, pp. 277–280.
[2] "Evolved universal terrestrial radio access (e-utra); physical channels and modulation (release 13)," in *Technical Specification 36.211 V13.13.0*, January 2020.
[3] J. Smith and J. Abel, "Closed-form least-squares source location estimation from range-difference measurements," *IEEE Transactions on Acoustics, Speech, and Signal Processing*, vol. 35, no. 12, pp. 1661–1669, 1987.
[4] X. Qu and L. Xie, "An efficient convex constrained weighted least squares source localization algorithm based on tdoa measurements," *Signal Processing*, vol. 119, pp. 142–152, 2016. [Online]. Available: https://www.sciencedirect.com/science/article/pii/S0165168415002583
[5] L. Zhang, T. Zhang, and H.-S. Shin, "An efficient constrained weighted least squares method with bias reduction for tdoa-based localization," *IEEE Sensors Journal*, vol. 21, no. 8, pp. 10 122–10 131, 2021.
[6] A. G. Venon, Y. Dupuis, P. Vasseur, and P. Merriaux, "Millimeter wave fmcw radars for perception, recognition and localization in automotive applications: A survey," *IEEE Transactions on Intelligent Vehicles*, pp. 1–1, 2022.
[7] X. Qu, L. Xie, and W. Tan, "Iterative source localization based on tdoa and fdoa measurements," in *2016 35th Chinese Control Conference (CCC)*, 2016, pp. 436–440.
[8] L. Cong and W. Zhuang, "Hybrid tdoa/aoa mobile user location for wideband cdma cellular systems," *IEEE Transactions on Wireless Communications*, vol. 1, no. 3, pp. 439–447, 2002.
[9] T. Jia, H. Wang, X. Shen, J. Gao, and X. Liu, "An accurate tdoa-aoa localization method using structured total least squares," in *OCEANS 2017 - Aberdeen*, 2017, pp. 1–6.
[10] H. Seo, H. Kim, J. Kang, I. Jeong, W. Ahn, and S. Kim, "3d moving target tracking with measurement fusion of tdoa/fdoa/aoa," *ICT Express*, vol. 5, 08 2018.
[11] X. Zhang, F. Wang, H. Li, and B. Himed, "Covariance-free tdoa/fdoa-based moving target localization for multi-static radar," in *2020 IEEE International Radar Conference (RADAR)*, 2020, pp. 901–905.
[12] R. Kaune, J. Hörst, and W. Koch, "Accuracy analysis for tdoa localization in sensor networks," in *14th International Conference on Information Fusion*, 2011, pp. 1–8.
[13] H. Liu, Y.-M. Pun, and A. M.-C. So, "Local strong convexity of maximum-likelihood tdoa-based source localization and its algorithmic implications," in *2017 IEEE 7th International Workshop on Computational Advances in Multi-Sensor Adaptive Processing (CAMSAP)*, 2017, pp. 1–5.
[14] E. I. P. Copa, K. Aziz, M. Rykunov, E. De Greef, A. Bourdoux, and F. Horlin, "Radar fusion for multipath mitigation in indoor environments," in *2020 IEEE Radar Conference (RadarConf20)*, 2020, pp. 1–5.
[15] H. Fang, N. Tian, Y. Wang, M. Zhou, and M. A. Haile, "Nonlinear bayesian estimation: from kalman filtering to a broader horizon," *IEEE/CAA Journal of Automatica Sinica*, vol. 5, no. 2, pp. 401–417, 2018.
[16] R. Schubert, E. Richter, and G. Wanielik, "Comparison and evaluation of advanced motion models for vehicle tracking," in *2008 11th International Conference on Information Fusion*, 2008, pp. 1–6.
[17] G. Jacovitti and G. Scarano, "Discrete time techniques for time delay estimation," *IEEE Transactions on Signal Processing*, vol. 41, no. 2, pp. 525–533, 1993.